

Evaluation of scanning tunneling spectroscopy data: Approaching a quantitative determination of the electronic density of states

B. Koslowski, C. Dietrich, A. Tschetschekin, and P. Ziemann

Abtl. Festkörperphysik, Universität Ulm, D-89069 Ulm, Germany

(Received 14 September 2006; revised manuscript received 27 November 2006; published 23 January 2007)

We introduce a method for recovering the electronic density of states (DOS) from scanning tunneling spectroscopy data. For this purpose, starting from one-dimensional WKB approximation, expressions are derived allowing the reconstruction of the DOS from a measured tunneling current (I - V curve) and its derivative with respect to the tunneling voltage, V . In a first step, assuming a constant DOS for the tip, I - V curves are calculated for various model DOS of the sample and the derived expressions are applied to recover the sample DOS. It turns out that in this way the original DOS can be recovered to an accuracy of some percent in the energy range ± 2 eV. In a second step, we rewrite the differential conductivity of the tunnel junction to form a Volterra integral equation of the second kind and, consequently, exploit the Neumann approximation scheme to optimize the recovered DOS for a wide class of original DOS to an unprecedented accuracy. In a third step, an energy-dependent DOS of the tip is included resulting in two Volterra integral equations, one for the sample and one for the tip DOS, allowing alternately optimizing the DOS of either side. By analyzing the distance dependence of spectroscopic data, i.e., the energy-resolved differential barrier height, we obtain additional information on the DOS which enables a self-consistent solution of the two integral equations and, thus, to deconvolute the sample and tip DOS.

DOI: [10.1103/PhysRevB.75.035421](https://doi.org/10.1103/PhysRevB.75.035421)

PACS number(s): 73.20.At, 68.37.Ef, 73.40.Gk

I. INTRODUCTION

Ever since the advent of scanning tunneling microscopy (STM) considerable efforts have been made to extend its power beyond taking topographic images with atomic resolution by analyzing the magnitude of the currents involved in the imaging process as well. In this way, additional information on the sample was expected to become available with the most basic of which being the electronic density of states (DOS). The theory of three-dimensional tunneling based on the transfer-Hamiltonian formalism¹ has been reexamined for STM purposes by several groups.²⁻⁵ Selloni *et al.*⁶ and Lang⁷ performed a theoretical analysis with special emphasis on scanning tunneling spectroscopy (STS), the experimental tool for revealing the DOS of a sample and/or tip. Nowadays software is freely available on the internet for calculating STM images and I - V curves.⁸ Partly by using *ab initio* methods, sample and tip are modeled by a specific atomic configuration and the tunneling current is calculated by applying a scattering theory. Data evaluation is then done by comparing theoretical and experimental topographic images as well as I - V or $\partial I/\partial V$ - V curves. Surprisingly, work on the recovery of the DOS from experimental data is rather scarce.

It was noticed early that $\partial I/\partial V$ - V curves or the differential conductivity – a widely used synonym for local density of states (LDOS) – are a rather poor measure of the DOS. To improve on this, experimentalists introduced normalizing these curves to their static conductivity, i.e., calculating $\partial \ln I/\partial \ln V$. In this way, $\partial I/\partial V$ - V curves taken at different tip-sample separations became more comparable and the highly dynamic background frequently observed in $\partial I/\partial V$ - V curves, especially on semiconductors,^{9,10} could be taken into account. Lang showed that the positions of peaks in $\partial \ln I/\partial \ln V$ - V curves correspond reasonably well to those in

the DOS shifting some ± 100 meV depending on the peak width of the DOS.^{7,11} Since the normalized conductivity tends to develop singularities if there is a gap in the DOS around the Fermi level, the normalization procedure had to be refined by introducing filter functions.^{12,13} Ukraintsev discussed this in detail and, finally, commented that due to all these empirical adjustments, it becomes increasingly difficult to judge the intrinsic value of the normalization procedure.¹⁴ In the same work, Ukraintsev proposed a technique for DOS deconvolution by normalizing the differential conductivity to its fitted asymmetric tunneling probability function based on the one-dimensional WKB approximation.¹⁴ Indeed, with the recently increasing interest in a quantitative analysis of tunneling spectra, the proposed technique led to promising results.¹⁵⁻²⁰

Nevertheless, the deconvolution introduced by Ukraintsev has its limitations. First, the DOS may also specifically contribute to the background of a $\partial I/\partial V$ - V curve which, however, the fit will attribute by principle to the tunneling probability function. Second, as will be shown in the present contribution, the calculation rests on an approximation which is not valid under typical tunneling conditions and the assumption of an *asymmetric* tunneling probability function is physically difficult to justify. Finally, the Ukraintsev approach leads to a deconvolution of the transmission probability and the DOS while the DOS is still a convolution of the DOS of the sample and the tip.

We approach the deconvolution of the transmission coefficient and the DOS in a different way. Assuming a WKB related transmission coefficient with parameters that can be reasonably estimated or determined from supplementary experiments such as the tunneling barrier height, which can be extracted from I - z curves, the *convoluted* DOS can be approximated by normalization of a quantity involving both,

the differential conductivity *and* the tunneling current, to the transmission coefficient. Exploiting the properties of a Volterra integral equation, this *convoluted* DOS can be further optimized to accurately reflect the measured data. Due to the symmetry of the tunneling junction, the sample DOS as well as the tip DOS fulfill a Volterra equation establishing a pair of coupled integral equations, which can be solved self-consistently if additional information on the DOS is available. Measurement of the bias-dependent differential barrier height is proposed to provide such independent information. We believe that the new method provides the experimentalist a reliable tool for accurately transposing the experimental data into the electronic density of states and potentially deconvolute the DOS of the tip and sample.

II. RECOVERING THE DOS: BASIC DERIVATION

The starting point of our calculation is the tunneling current, I , as given by the one-dimensional WKB approximation for a barrier characterized by an energy dependent transmission coefficient $T(E)$. Accordingly, applying a bias, V , between the right and left side of the barrier leads to a tunneling current, which reads^{4,14,21}

$$I(V) = \int_{-\infty}^{\infty} \rho_S(E) \rho_T(E - V) T(E, V) f_{12}(E, V) dE, \quad (1)$$

where ρ_S and ρ_T are the sample and tip density of states (DOS), respectively, f_{12} is a window function $f_{12}(E, V) = f(E - V) - f(E)$ with the Fermi-Dirac distribution f . Here, atomic (Hartree) units are used with all constants set to unity including the effective tip-surface contact area, and the problem is described in the reference frame of the sample with the energy measured with respect to the Fermi level of the sample. Note, that, in general, the DOS used in Eq. (1) is not the total DOS as determined from band structure calculations but a weighted DOS if a certain selectivity of tunneling in k space is present. According to the one-dimensional WKB approximation the transmission coefficient at zero bias is given by $T(E) = e^{-\sqrt{\Phi - E}z}$ with z being the tip-sample distance and Φ the effective tunneling barrier height. A bias dependence of the transmission coefficient is included by the trapezoidal approximation leading to $T(E, V) = e^{-\sqrt{\Phi + V/2 - E}z}$. For quick reference, the barrier together with the various energies is sketched in Fig. 1. To allow for a more general treatment of the bias dependence of the barrier, the factor $1/2$ in the square root argument of $T(E, V)$ is replaced in the following by $1/\alpha$ with α being a number close to 2, which has to be determined experimentally from bias dependent barrier measurements. We calculate the derivative of the tunneling current and obtain

$$\partial_V I(V) = \int_{-\infty}^{\infty} \rho_S(E) \partial_V [\rho_T(E - V) T(E, V) f_{12}(E, V)] dE \quad (2a)$$

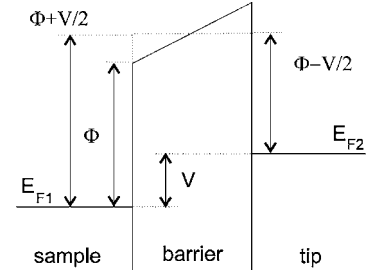


FIG. 1. Energy diagram of a tunneling junction including an applied bias. The symbols are: the Fermi energy of the sample and tip, E_{F1} , E_{F2} , respectively, the barrier height Φ , and the applied bias V (here in eV).

$$\begin{aligned} &\approx \rho_S(V) \rho_T(0) T(E = V) - \int_{-\infty}^{\infty} \rho_S(E) \rho_T(E - V) \\ &\times T(E, V) f_{12}(E, V) \frac{z}{2\alpha \sqrt{\Phi + \frac{V}{\alpha} - E}} dE \\ &+ \int_{-\infty}^{\infty} \rho_S(E) T(E, V) f_{12}(E, V) \partial_V \rho_T(E - V) dE, \end{aligned} \quad (2b)$$

where the \approx sign is due to the approximation $\partial_V f_{12}(E, V) \approx \delta(E - V)$, which is widely used in solid state physics if the involved Fermi-Dirac distributions are taken at room temperature. Furthermore, another key relation was exploited which apparently has been overlooked in related previous works

$$\partial_V T(E, V) = \frac{-z}{2\alpha \sqrt{\Phi + \frac{V}{\alpha} - E}} T(E, V). \quad (2c)$$

Due to the square-root appearing in the denominator, the second term on the right side of (2b) becomes singular for $E = \Phi + V/\alpha$. We ignore this problem since we can circumvent it by using the zero temperature approximation of (1) with finite boundaries of the integral and choosing V sufficiently small compared to Φ thereby avoiding the field-emission regime. Note that $\partial_V T(E, V) = -\frac{1}{\alpha} \partial_E T(E, V)$ for the specific transmission coefficient given above, which however, will not be used in the following analysis for the sake of generality.

For now, we set the tip density of states to unity, $\rho_T = 1$, and, hence, $\partial_V \rho_T$ vanishes. Then, the third term on the right of (2b) vanishes resulting in

$$\begin{aligned} \partial_V I(V) &\approx \rho_S(V) T(E = V) \\ &- \int_{-\infty}^{\infty} dE \rho_S(E) T(E, V) f_{12}(E, V) \frac{z}{2\alpha \sqrt{\Phi + \frac{V}{\alpha} - E}}. \end{aligned} \quad (3)$$

At this point, one usually neglects the second term leading to the well-known and simple result $\partial_V I(V) \propto \rho_S(V)$.¹⁴ However, it can easily be shown that the second term is comparable to the first and should not be neglected at all. Comparing the argument of the integral in Eq. (3) with the corresponding argument in Eq. (1) shows its identity except for an additional slowly varying factor $z/2\alpha\sqrt{\Phi + \frac{V}{\alpha} - E}$. Applying the generalized mean value theorem for integrals and setting the mean value to $\frac{z}{2\alpha\sqrt{\Phi}}$ delivers

$$\partial_V I(V) \approx \rho_S(V)T(E=V) - \frac{z}{2\alpha\sqrt{\Phi}}I(V). \quad (4)$$

Since we are interested in the DOS of the sample, ρ_S , we solve (4) for ρ_S and obtain

$$\rho_{Se}(V) = \frac{1}{T(E=V)} \left(\partial_V I(V) + \frac{z}{2\alpha\sqrt{\Phi}}I(V) \right), \quad (5a)$$

where we added the index “e” to indicate that, in a practical application of tunneling, ρ_{Se} is the DOS recovered from an experimentally determined tunneling current and its derivative. In the above derivation, it was assumed that the singularity at $E = \Phi + V/\alpha$, which might be met in the regime of the field emission, is definitely avoided in the corresponding experiment as well as, of course, in the numerical treatments.

Relation (5a) is especially interesting since it manifests a dependence of tunneling spectroscopy on the tip-sample separation which has already been proposed earlier to yield additional information.^{6,14} According to Eq. (5a), the derivative, $\partial_V I$, carries the full spectroscopic information at small tip-sample separation only. With increasing separation, however, the spectroscopic information shifts to the tunneling current due to the growing influence of the energy dispersivity of the tunneling barrier [cf. (2c)]. Theoretically, this separation dependence offers the opportunity to determine the *absolute* tip-sample separation by comparing I - V spectra measured at sufficiently different z values. A tip-sample interaction or, in practice, a limited precision of the measurement or a limited range of the separation could preclude that possibility.

In a typical STM experiment, values of z and Φ are 7 Å and 4 eV, respectively, leading to $\frac{z}{2\alpha\sqrt{\Phi}} \approx 1$. Thus, the tunneling current contributes equally to the recovered DOS of the sample as the derivative of the tunneling current does. From an experimental point of view, the important aspect of Eq. (5a) is that we have exclusively known parameters on its right side: The tunneling barrier height, Φ , and α can be determined experimentally and, hence, the transmission coefficient is known from the WKB approximation. Similarly, the tip-sample separation, z , can be derived from the experiment due to the separation dependence of tunneling spectra or by a gentle touch of the sample surface with the tunneling tip.

The work of Ukraintsev¹⁴ is based on Eq. (5a) with $z=0$, i.e., neglecting the term containing the tunneling current. Consequently, a modification of the transmission coefficient, T , is required to recover a meaningful DOS. Since predomi-

nantly occupied states at the Fermi level of the tip probe empty states of the sample at positive bias, and occupied states at the Fermi level of the sample probe empty states of the tip at negative bias, replacement of a single transmission coefficient by a sum of two, one for the tip and one for the sample, could be justified. We will use this “symmetry argument” later.

We finally refine (5a) by calculating the mean value analytically for a *constant* DOS of the sample and apply a second order approximation. In this way, one arrives at

$$\rho_{Se}(V) = \frac{1}{T(E=V)} \times \left[\partial_V I(V) + \frac{z}{2\alpha\sqrt{\Phi}} \left(1 + \frac{(2\sqrt{\Phi}z + 3)V^2}{96\Phi^2} \right) I(V) \right]. \quad (5)$$

To illustrate the effect of this approximation, we calculate the tunneling current, I , its derivative, $\partial_V I$, and the approximated DOS of the sample, ρ_{Se} , for *constant* DOS of the sample, $\rho_S=1$. For comparison, we have also calculated the normalized conductivity $\frac{V}{I} \frac{\partial I}{\partial V}$. The results are shown in Fig. 2(a). In the wide energy range of ± 2 eV, the tunneling behavior exhibits the well known parabolic conductivity [dash-dotted curve in Fig. 2(a)]. The normalized conductivity [dashed curve in Fig. 2(a)] reduces the parabolic component by about 50% but still it is clearly present and, thus, is similarly unsuitable for a satisfactory determination of the sample’s DOS as is the derivative of the tunneling current, $\partial_V I$. The approximated DOS of the sample, ρ_{Se} , however, recovers the constant input DOS to an accuracy of $+0.5/-0.2\%$ in the energy range ± 1 eV and $+0.8/-10\%$ in the energy range ± 2 eV [solid curve in Fig. 2(a)]. For positive bias, the deviation of ρ_{Se} is almost constant and almost independent of the bias while, for negative bias, the error increases rapidly with decreasing bias. This is due to the fact that the current, I , is an odd function of the bias and its derivative, $\partial_V I$, is even. As consequence, the function in parenthesis on the right of (5) is large for positive bias and becomes very small for negative bias [approximately as $T(E=V) = e^{-\sqrt{\Phi+V/\alpha-V}z}$]. An error due to the parabolic approximation in (5) has, hence, a more vigorous impact on the result for negative bias than for positive bias. Note, that the result of Ukraintsev’s approach would be unity to a very good accuracy in the given special case.

At this point, the physical meaning of Eq. (5) should be emphasized again. In general, I - V curves determined by tunneling reflect the influence of both, structure in the DOS as well as a voltage and energy dependent barrier transmission.²² To separate these different contributions, for the derivation of Eq. (5) the trapezoidal approximation for the barriers has been explicitly assumed together with constant DOS for tip and sample. As a consequence, starting with a supposed constant sample DOS, Eq. (5) consistently recovers this model DOS as opposed to $\partial_V I$ and $\partial \ln I / \partial \ln V$ when directly interpreted as DOS without considering the effect of the barrier. In that case, the barrier effect shows up

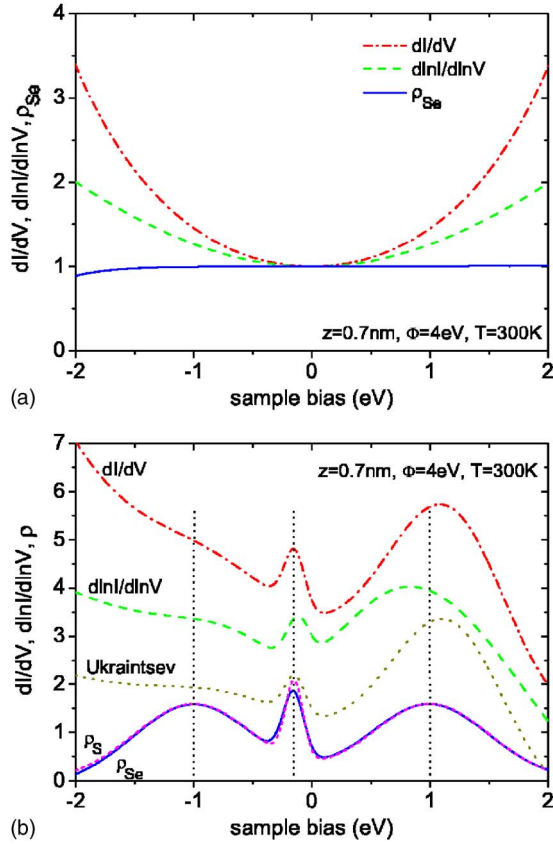


FIG. 2. (Color online) Calculated derivative of the tunneling current, $\partial_V I$, normalized conductivity $\partial \ln I / \partial \ln V$, the result of Ukraintsev's approach [in (b) only] and the approximated DOS of the sample, ρ_{Se} , as a function of the applied bias, V , for constant tip density of states, $\rho_T=1$, at temperature $T=300$ K. Panel (a) presents the calculation for constant sample density of states, $\rho_S=1$; panel (b) presents the calculation for a sample density of states being composed of three Gaussian peaks: two peaks at ± 1 eV of full width at half maximum (FWHM) 1 eV and area $A_{\pm 2}=2$, and one Gaussian peak at -0.15 eV of FWHM 0.15 eV and area $A_{-0.15}=0.3$. For comparison, the original DOS, ρ_S , is also shown in panel (b). In panel (b), the curves Ukraintsev, $\partial \ln I / \partial \ln V$ and $\partial_V I$ have been offset for clarity by 1, 2, 3, respectively. ($\Phi=4$ eV, $z=7$ Å, $\alpha=2$).

as DOS leading to obvious misinterpretations as pointed out recently by Olsson *et al.*²² The question then arises whether the barrier approximation included in Eq. (5) is sufficient when assuming a more complicated model DOS for the sample. This is tested for a sample DOS comprised of three Gaussian peaks centered at $-1/-0.15/+1$ eV (area 2/0.3/2 and width 1.0/0.15/1.0 eV), respectively [Fig. 2(b)]. This model DOS varies by about one order of magnitude over the bias range of ± 2 eV [short dashed curve in Fig. 2(b)]. The calculated derivative $\partial_V I$ [dash-dotted curve in Fig. 2(b)], the normalized conductivity $\partial \ln I / \partial \ln V$ [dashed curve in Fig. 2(b)] as well as the result of Ukraintsev's approach [UA, dotted curve in Fig. 2(b)] produce a peak close to $+1$ eV, shifted by $+0.1$ eV in $\partial_V I$ and UA, and -0.2 eV in $\partial \ln I / \partial \ln V$. The conductivity and consequently the normalized conductivity and UA become negative for $V > 1.8$ eV

prohibiting a Gaussian fit at positive bias to either curve. All three curves regenerate the thermally broadened peak close to -0.15 eV with a shift of 30 meV to -0.12 eV in $\partial \ln I / \partial \ln V$. All three curves, $\partial_V I$, UA and $\partial \ln I / \partial \ln V$, deliver just a shoulder at -1 eV rather than the original peak positioned there. It is obvious from these curves that a quantitative analysis of a sample's DOS is impossible by just analyzing $\partial_V I$, $\partial \ln I / \partial \ln V$, or UA. At the very best, one may obtain some qualitative hints as to the presence of structure in the DOS. In contrast to the failure of $\partial_V I$, $\partial \ln I / \partial \ln V$ and UA in this respect, the recovered DOS of the sample according to Eq. (5), ρ_{Se} , regenerates the original DOS with a surprising accuracy [solid curve in Fig. 2(b)]. Fitting three Gaussian functions to ρ_{Se} recovers the peak positions to an accuracy of ± 6 meV corresponding to one bias step in the calculation (5 meV). The areas of the peaks are recovered to an accuracy of better than 4% for negative bias and better than 1% at positive bias. The model peak at -0.15 eV was found significantly broadened by 33 meV due to thermal smearing at $T=300$ K. Consistently, the peak appears reduced in height but with the total area conserved.

Though the calculation presented above has demonstrated a significant improvement over earlier considerations, Eq. (5) has been derived under the assumptions of the trapezoidal approximation describing the barrier transmission sufficiently well or, expressed alternatively, that the function in front of the I - V contribution in Eq. (5) represents an adequate choice of the mean value needed to approximate the integral in the starting Eq. (3). Additionally, a constant tip DOS was assumed. If, however, the DOS of the sample varies too strongly over the considered bias range, Eq. (5) may turn out as only a rather rough estimate because the mean value may then be a function of ρ_S itself. As experienced above, this primarily leads to errors at negative bias. The following considerations show how to remedy this deficiency numerically.

III. RECOVERING THE DOS: NUMERICAL IMPROVEMENTS

Equation (3) can be rewritten in the form of a Volterra integral equation of the second kind to obtain

$$\rho_S(V) = \frac{\partial_V I(V)}{T(E=V)} + \frac{z}{2\alpha} \int_0^V \frac{T(E,V)}{\sqrt{\Phi + \frac{V}{\alpha} - ET(E=V)}} \rho_S(E) dE. \quad (6)$$

For simplicity we have employed here the zero temperature approximation for the tunneling current introducing finite limits of the integral. This, however, is no serious restriction, since in the numerical treatment of Eq. (6) the window function $f_{12}(E,V)$ as well as an extension of the upper limit of the integral can be easily included if only this limit stays well below the singularity at $E=\Phi+V/\alpha$. Within these limits, the integral kernel in Eq. (6) is continuous and, thus, the Volterra integral equation can be solved numerically by Neumann's approximation scheme delivering the series

$$\rho_{S,n}(V) = \frac{\partial_V I(V)}{T(E=V)} + \frac{z}{2\alpha} \int_0^V \frac{T(E,V)}{\sqrt{\Phi + \frac{V}{\alpha} - ET(E=V)}} \rho_{S,n-1}(E) dE = \frac{1}{T(E=V)} \left(\partial_V I(V) + \frac{z}{2\alpha} \int_0^V \frac{T(E,V)}{\sqrt{\Phi + \frac{V}{\alpha} - E}} \rho_{S,n-1}(E) dE \right). \quad (7)$$

As input function $\rho_{S,1}$ one starts with $\partial_V I$ or $\partial_V I/T(E,V)$, respectively. We use here the approximation, ρ_{Se} , of ρ_S which leads to a much faster convergence of $\rho_{S,n}$ towards the numerical solution, ρ_{Sr} , obtained by iteratively applying Eq. (7) to the DOS of the sample, $\rho_{S,n}$.

To demonstrate this iterative procedure, in Fig. 3 its result is presented for an assumed steplike DOS of the sample, ρ_S , represented by a Heavyside step function centered at -0.5 eV. Such a DOS can be considered as being a model of the Shockley-like surface state of Au(111). Calculation of $\partial_V I$, UA, and $\partial \ln I / \partial \ln V$ with a barrier height of $\Phi=4$ eV and $T=300$ K delivers the dash-dotted, dashed, and dotted curves in Fig. 3. In all three cases, only a strongly reduced step at $V=-0.5$ eV is recovered on a background with a step height exhibiting roughly the same magnitude as this background. Thus, similar to the result presented in Fig. 2(b), all three types of tunneling data, $\partial_V I$, UA and $\partial \ln I / \partial \ln V$, which are most often interpreted as DOS, are not suitable to quantitatively recover the given steplike ρ_S . Next, the first approximation, $\rho_{S,1}=\rho_{Se}$, of the above iterative approach is calculated with $z=0.7$ nm according to Eq. (5). The result is added to Fig. 3 as solid curve. As an obvious improvement, the recovered DOS, ρ_{Se} , regenerates accurately the thermally smeared step from zero left of the step to the constant value of unity right of the step. For decreasing bias, however, ρ_{Se} increases to ~ 0.33 instead of staying at zero. Apparently, the approximation of the mean value is too rough for this choice of the sample's DOS. By applying, however, only 5 itera-

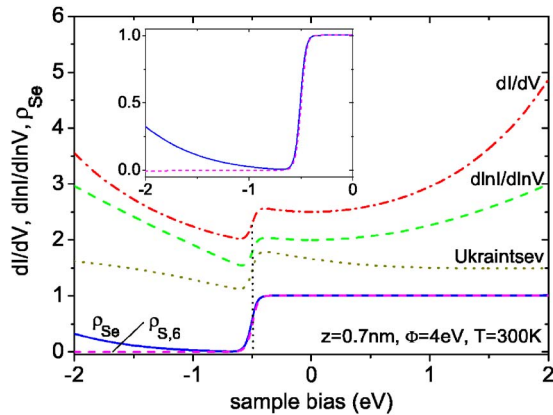


FIG. 3. (Color online) Effect of applying Neumann's approximation scheme to the approximated sample density of states for $\rho_T=1$. The original density of states, ρ_S , is a step function $\rho_S(E) = \Theta(E+0.5 \text{ eV})$ as a model for the Shockley-like surface state of Au(111). The inset is a zoom-in to the area of interest. The curves Ukraintsev, $\partial \ln I / \partial \ln V$ and $\partial I / \partial V$ have been offset for clarity by 0.5, 1.0, and 1.5, respectively. ($\Phi=4$ eV, $z=7 \text{ \AA}$, $\alpha=2$, $T=300$ K).

tions according to Eq. (6), the DOS, $\rho_{S,n}$, approaches closely its final value with $|\rho_{S,6}| < 0.007$ for $V < -0.5$ eV. A residual deviation from zero left of the step or from unity right of the step comes from numerical errors performing the integration and differentiation.

It is worth mentioning that the above procedure is equally well suited for DOS recovery of a semiconductor. Modeling the semiconductor DOS as unity outside and zero inside the gap at ± 1 eV and disregarding effects like band bending, the approximated DOS, ρ_{Se} , regenerates the conduction band with an accuracy of better than 1% and the valence band edge with an accuracy of 2% while the DOS is falling off to 0.75 at -2 eV. Yet, after 5 iterations, the recovered DOS, $\rho_{S,6}$, fits the original DOS to an accuracy of $-0/+0.7\%$ (disregarding the thermal broadening of the band edges).

IV. INCLUSION OF THE TIP DOS

Though the above formalism appears promising, inclusion of an energy dependent DOS of the tip would be highly desirable. For this purpose, the above principal derivation is reanalyzed first for an arbitrary tip DOS, $\rho_T(E)$, followed by an attempt to generalize the numerical procedure to optimize $\rho_{S,n}$ as well as $\rho_{T,n}$.

When keeping a tip DOS depending on the energy, Eq. (3) reads

$$\partial_V I(V) = \rho_S(V) \rho_T(0) T(E=V) - \int_{-\infty}^{\infty} dE \rho_S(E) T(E,V) f_{12}(E,V) \times \left(\frac{z \rho_T(E-V)}{2\alpha \sqrt{\Phi + \frac{V}{\alpha} - E}} + \partial_E \rho_T(E-V) \right), \quad (8)$$

where we used $-\partial_V \rho_T(E-V) = \partial_E \rho_T(E-V)$. The corresponding Volterra integral equation becomes

$$\rho_S(V) = \frac{1}{\rho_T(0) T(E=V)} \left[\partial_V I(V) + \int_0^V dE T(E,V) \times \left(\frac{z \rho_T(E-V)}{2\alpha \sqrt{\Phi + \frac{V}{\alpha} - E}} + \partial_E \rho_T(E-V) \right) \rho_S(E) \right]. \quad (9)$$

Equation (9) is the Volterra integral equation for the sample's DOS. To obtain the analog for the tip DOS, we change the reference frame from the sample to the tip. This leads to an identical equation with, however, interchanged indices of the DOS. Bearing in mind, that the current measured at the

tip is the negative current measured at the sample, and that the bias at the sample corresponds to a negative bias at the tip, we find $V_T = -V$, $I_T(V_T) = -I(V) = -I(-V)$, $\partial_{V_T} I_T(V_T) = \partial_V I(-V)$ with the index “ T ” indicating that the quantity is measured with respect to the reference frame of the tip. The Volterra integral equation for the DOS of the tip then reads

$$\rho_T(V_T) = \frac{1}{\rho_S(V_T=0)T(E=V_T)} \left[\partial_V I(-V_T) + \int_0^{VT} dE T(E, V_T) \times \left(\frac{z\rho_S(E-V_T)}{2\alpha\sqrt{\Phi + \frac{V_T}{\alpha} - E}} + \partial_E \rho_S(E-V_T) \right) \rho_T(E) \right]. \quad (10)$$

Note, that this equation is identical to Eq. (9) in the respective reference frame but $\partial_V I$ must be mirrored at $V=0$ because $\partial_V I$ has been measured in the reference frame of the sample. This is very convenient for the numerical calculation, since the same routine can be used in both cases by just interchanging the role of ρ_S and ρ_T and taking the mirror image of $\partial_V I$.

Two procedures of finding separately the DOS of the tip and the sample from the tunneling current and its derivative are conceivable. The first is determining the tip DOS for a specific tip at a given DOS of a suitable calibration sample and from that determine an unknown sample DOS. However, this type of calibration would be successful only if the stability of the tip could be guaranteed over a sufficient period of time. A second procedure is based on solving alternately the integral equations for the sample and the tip. In general, without further information the result is obviously not unique. Improvement, however, can be accomplished if additional information on the DOS is available which allows checking the DOS for self-consistency in the course of iteration. A first step towards this direction could be a comparative tunneling spectroscopy study, i.e., comparison of tunneling spectra obtained at different sites of a sample, and solving the set of pairs of integral equations under the condition that the DOS of the tip is the same in all integral equations. A more promising possibility, however, is based on the separation dependence of tunneling spectroscopy and will be described in the following section.

V. THE DIFFERENTIAL BARRIER HEIGHT

The set of coupled integral equations (9) and (10) could be solved self-consistently if independent information on the DOS was available. For that purpose one may harness the separation dependence of $\partial I/\partial V$ spectra. Figure 4(a) illustrates the separation dependence of tunneling spectra for a specific combination of sample and tip DOS. The sample DOS is unity plus two Gaussian peaks at ± 1 eV (width 0.1 eV, area 0.2) and the tip DOS comprises three Gaussian peaks at ± 1.3 eV and 0 eV (width 1 eV, area 1.33) [compare lower inset of Fig. 4(a)]. Shown are calculated $\partial I/\partial V$ - V curves for tip-sample separations of 0.1, 0.3, 0.5, and 0.7 nm. The $\partial I/\partial V$ - V curves have been normalized to their zero-bias conductivity for better comparison. The two peaks

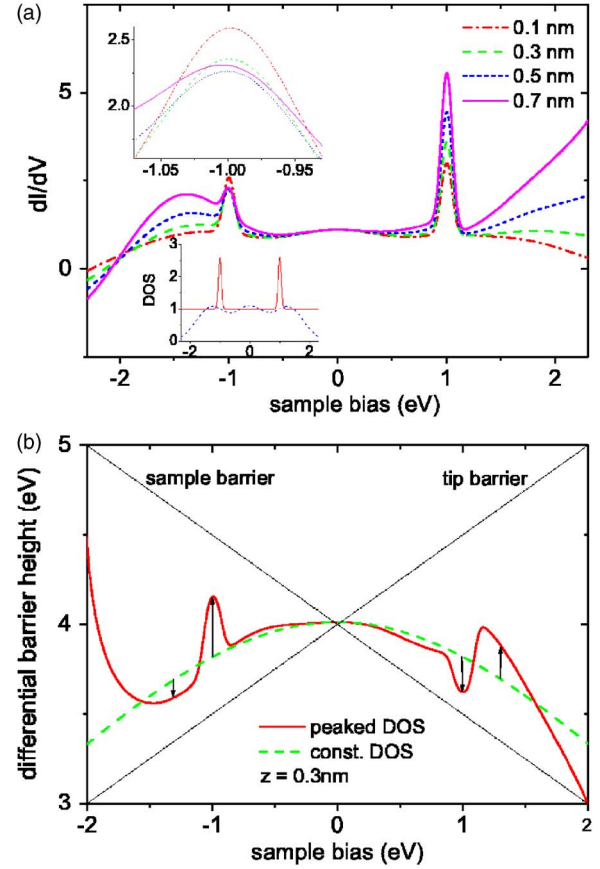


FIG. 4. (Color online) (a) Separation dependent $\partial_V I$ curves calculated for a sample DOS composed of two Gaussian peaks centered at ± 1 eV (width 0.1 eV, area 0.2) on top of a constant background of unity height and a tip DOS comprising 3 Gaussians centered at ± 1.3 eV and 0 eV (width 1 eV and area 1.33 each) (lower left inset, $T=0$ K). The upper left inset is a close-up of the $\partial_V I$ curves at -1 eV emphasizing the separation behavior opposite to that observed for the peak at $+1$ eV. For better comparison the spectra have been normalized to their zero conductivity. ($\Phi = 4$ eV, $\alpha = 2$). (b) The differential barrier height $(\partial_z \partial_V I / \partial_V I)^2$ calculated by numerically differentiating $\partial_V I$ for the same DOS as in (a) for $z = 0.3$ nm. The dashed curve represents $(\partial_z \partial_V I / \partial_V I)^2$ for sample and tip DOS set equal to unity and $z = 0.3$ nm. The straight lines correspond to the barrier height experienced by states of the sample at energy $E = V$ ($\Phi - V/2$) and by states of the tip at energy $E = -V$ ($\Phi + V/2$). ($\Phi = 4$ eV, $\alpha = 2$, $T = 0$ K).

in the $\partial I/\partial V$ - V curves at ± 1 eV reflect the two peaks in the sample DOS, which, however, were constructed with identical intensities. On the other hand, the calculated peaks exhibit clearly different intensities with the one at $+1$ eV significantly higher than the other at -1 eV. This difference can be traced back to the behavior of the transmission coefficient, which is higher for sample states at higher energy. Furthermore, the peak at $+1$ eV increases with increasing tip-sample separation because the transmission coefficient at $V = E = 0$ eV [$T(E = V = 0) = e^{-\sqrt{\Phi}z}$], at which the plotted curves have been normalized, decreases faster with increasing separation than at $V = E = 1$ eV [$T(E = V = 1) = e^{-\sqrt{\Phi+1}z}$]. The analogous argument explains the decrease of the peak at -1 eV. For tip states, however, the

situation is exactly opposite: unoccupied states ($E > 0$) appear at negative bias but experience a higher transmission coefficient and, consequently, show stronger separation dependence for $V < 0$ than for $V > 0$. This expectation is clearly corroborated by the peaks at -1.3 eV and $+1.3$ eV, respectively. Note that the apparent reversal of the peak height at -1.0 eV for 0.7 nm [solid curve in the upper left inset of Fig. 4(a)] is due to the increasing peak at -1.3 eV.

The separation dependence can be analyzed further by numerically calculating the derivative of $\partial_V I$ with respect to separation z , $\partial_z \partial_V I$, normalized to $\partial_V I$. The square of this quantity, $(\partial_z \partial_V I / \partial_V I)^2$, is a measure of the barrier height and will be called differential barrier height, $\hat{\Phi}$. Note that $\hat{\Phi}$ is similar to the commonly used definition of the barrier height $(\partial_z I / I)^2$ which, in general, exhibits no significant voltage dependence and, hence, is approximately given by $(\partial_z I / I)^2 = \Phi$ independently of the tunneling bias. On the other hand, $\hat{\Phi}$ selects especially the states at the Fermi levels as will be shown below. In Fig. 4(b) we display the differential barrier height, $\hat{\Phi}$, calculated numerically from the data shown in Fig. 4(a) at a tip-sample separation of 0.3 nm (solid curve). Added to this panel are the differential barrier height for constant tip and sample DOS at the same separation (dashed curve) as well as the barrier heights for states at the Fermi levels of the tip and sample, respectively (solid straight lines).

It is obvious from Fig. 4(b) that $\hat{\Phi}$ for the peaked model DOS deviates from the differential barrier height for constant DOS. Additionally, closer inspection shows that these deviations exhibit a clear trend: $\hat{\Phi}$ shifts towards the sample barrier²³ if the sample DOS outweighs the tip DOS with respect to zero bias, and vice versa. This way, one obtains additional information about how the DOS of tip and sample are related to each other at a given energy with respect to zero bias.

To corroborate the above idea, we calculate analytically the derivative $\partial_z \partial_V I$ for constant tip and sample DOS, $\rho_S = \rho_T = 1$, and normalize it with respect to the zero-bias transmission coefficient. This gives

$$\partial_z \partial_V I_n = -\frac{1}{2e^{-\sqrt{\Phi}z}} \left(\sqrt{\Phi - \frac{V}{2}} e^{-\sqrt{\Phi - V/2}z} + \sqrt{\Phi + \frac{V}{2}} e^{-\sqrt{\Phi + V/2}z} \right). \quad (11)$$

This can be interpreted as $\partial_z \partial_V I_n$ being just the weighed average of the inverse decay length for states at the Fermi level of the tip, probing states of the sample at energy $E = V$ [first term in (11)], and for states at the Fermi level of the sample, probing states of the tip at energy $E = -V$ [second term in (11)]. An example of $(\partial_z \partial_V I_n)^2$ is shown in Fig. 4(b) (dashed curve).

The weight of the states at the respective Fermi levels is given by the relative transmission with respect to its zero-bias value. We adopt this argument and generalize (11) to include the DOS being variable in energy and obtain

$$\begin{aligned} \partial_z \partial_V I_n = & -\frac{e^{\sqrt{\Phi}z}}{2\rho_S(0)\rho_T(0)} \left(\sqrt{\Phi - \frac{V}{2}} e^{-\sqrt{\Phi - V/2}z} \rho_S(V) \rho_T(0) \right. \\ & \left. + \sqrt{\Phi + \frac{V}{2}} e^{-\sqrt{\Phi + V/2}z} \rho_S(0) \rho_T(-V) \right). \quad (12) \end{aligned}$$

Equation (12) establishes a direct functional relation between the DOS of the sample and the DOS of the tip by means of the experimentally determined relation $\partial_z \partial_V I / \partial_V I$ which can be used to check the recovered DOS for self-consistency. Note that the proposed procedure fails for large tip-sample separation since in that case $\partial_z \partial_V I / \partial_V I$ approaches the tip or sample barrier, whichever is smaller, and even a considerable change of the DOS will lead to only a small change of the differential barrier. Note also that the self-consistency check could be hampered in practice by a limited precision of measured data and the limited accessible range in tip-sample separation concomitantly with effects not included in our consideration like, e.g., a tip-sample interaction or a separation dependent barrier height.

VI. EXTENSIONS

The above considerations rest on the assumption of an explicit transmission coefficient, T . This led to Eqs. (4) and (5) by taking the derivative of T allowing to apply the mean value theorem with the remaining integral being the experimentally accessible tunneling current, I . The only requirement to be met by a transmission coefficient is being invariant under taking its derivative with respect to V . This is particularly the case if T is an exponential. The only change required when using an alternative transmission coefficient is to adjust the mean value accordingly.

We exemplify this by extending the calculation for a surface state like the one on Au(111) (Fig. 3) or Cu(111) to three-dimensional tunneling. The three-dimensional transmission coefficient, T_3 , depends only on the energy component perpendicular to the tunneling barrier, $E_{\perp} = E - E_{\parallel}$. Due to the almost perfect parabolic dispersion of the surface state, E_{\perp} is simply $E_{\perp} = E_0$ with E_0 being the band onset ($E_0 = -0.47$ eV for gold). The transmission coefficient is then $T_3(V) = e^{-\sqrt{\Phi + V/\alpha - E_0}z}$ which no longer depends on the independent variable, E . The resulting $\partial I / \partial V - V$ curve is very similar to the $\partial I / \partial V - V$ curve calculated for Cu(111) and a Ni tip in Ref. 21. Equation (3) can be solved analytically and (5a) becomes

$$\rho_S(V) = \frac{1}{T_3(V)} \left(\partial_V I(V) + \frac{z}{2\alpha \sqrt{\Phi + \frac{V}{\alpha} - E_0}} I(V) \right), \quad (13)$$

where we omitted the suffix “ e ” on the left side since this is now an analytical expression with no approximations.

VII. CONCLUSION

On the basis of the one-dimensional WKB approximation, we introduced a new method of analyzing spectroscopic data in scanning tunneling spectroscopy. This analysis enables us to principally recover the density of states of a sample semi-quantitatively and it allows us to deconvolute the DOS of tip and sample. The new method comprises three components: (1) determination of an approximate DOS of the sample assuming a constant DOS of the tip. The approximated DOS is superior to previous approximations because it includes con-

tributions which have been improperly neglected before. (2) Numerical improvement of the approximated DOS by treating the underlying equation as a Volterra integral equation and applying Neumann's approximation scheme. The obtained solution recovers the input DOS to an accuracy of better than 1% after only 5 iterations and allows a quantitative comparison of features in the DOS all over the considered bias range. (3) We have included an energy-dependent DOS of the tip and obtained a set of two coupled Volterra integral equations for the DOS of the sample and the tip, respectively. In order to support deconvolution of the two densities of states we derived a relation for both DOS which can be resolved experimentally by differential barrier measurements. With this additional constraint on the DOS the system of two coupled integro-differential equations could be solved self-consistently.

Though we performed the calculations for a specific transmission coefficient derived from the one-dimensional WKB approximation, the presented formalism is more general. The only pre-conditions for the formalism to work are a transmission coefficient being invariant under taking its derivative with respect to the tunneling bias and the validity of the WKB approximation. We showed this by extending the formalism to three-dimensional tunneling into Shockley-like surface states as on Au(111).

ACKNOWLEDGMENTS

We gratefully acknowledge financial support by the Deutsche Forschungsgemeinschaft (DFG, collaborative research center SFB 569). We also thank O. Marti for valuable discussions.

-
- ¹J. Bardeen, Phys. Rev. Lett. **6**, 57 (1961).
²J. Tersoff and D. R. Hamann, Phys. Rev. Lett. **50**, 1998 (1983); Phys. Rev. B **31**, 805 (1985).
³N. Garcia, C. Ocal, and F. Flores, Phys. Rev. Lett. **50**, 2002 (1983).
⁴T. E. Feuchtwang, P. H. Cutler, and N. M. Miskovsky, Phys. Lett. **99A**, 167 (1983).
⁵N. D. Lang, Phys. Rev. Lett. **55**, 230 (1985); N. D. Lang, *ibid.* **55**, 2925 (1985); N. D. Lang, *ibid.* **56**, 1164 (1986).
⁶A. Selloni, P. Carnevali, E. Tosatti, and C. D. Chen, Phys. Rev. B **31**, 2602 (1986).
⁷N. D. Lang, Phys. Rev. B **34**, 5947 (1986).
⁸<http://www.icmm.csic.es/jcerda/>; <http://www.flapw.de/>; <http://cms.mpi.univie.ac.at/vasp/>
⁹J. A. Stroscio, R. M. Feenstra, and A. P. Fein, Phys. Rev. Lett. **57**, 2579 (1986).
¹⁰J. A. Stroscio and R. M. Feenstra, in *Scanning Tunneling Microscopy*, edited by J. A. Stroscio and W. J. Kaiser, *Methods of Experimental Physics*, Vol. 27 (Academic, New York, 1993).
¹¹The tunneling parameters (barrier height and tip-sample separation) may also play a role.
¹²P. Mårtensson and R. M. Feenstra, Phys. Rev. B **39**, 7744 (1989).
¹³R. M. Feenstra, Phys. Rev. B **50**, 4561 (1994).
¹⁴V. A. Ukraintsev, Phys. Rev. B **53**, 11176 (1996).
¹⁵T. K. Yamada, R. Robles, E. Martinez, M. M. J. Bischoff, A. Vega, A. L. Vazquez de Parga, T. Mizoguchi, and H. van Kempen, Phys. Rev. B **72**, 014410 (2005).
¹⁶J. Mitra, Mandar Paranjape, A. K. Raychaudhuri, N. D. Mathur, and M. G. Blamire, Phys. Rev. B **71**, 094426 (2005).
¹⁷J. K. Garleff, M. Wenderoth, K. Sauthoff, R. G. Ulbrich, and M. Rohlffing, Phys. Rev. B **70**, 245424 (2004).
¹⁸T. Andreev, I. Barke, and H. Hövel, Phys. Rev. B **70**, 205426 (2004).
¹⁹M. Prutzer and H. J. Elmers, Phys. Rev. B **69**, 134418 (2004).
²⁰J. Mitra, A. K. Raychaudhuri, Ya M. Mukovskii, and D. Shulyatev, Phys. Rev. B **68**, 134428 (2003).
²¹G. Hörmandinger, Phys. Rev. B **49**, 13897 (1994).
²²F. E. Olsson, M. Persson, J. Repp, and G. Meyer, Phys. Rev. B **71**, 075419 (2005).
²³i.e., the barrier height experienced by states of the sample at energy $E=V$ aligned with the Fermi level of the tip.